Chapter 2
Earthquake Resilience of High-Rise Buildings: Case Study of the 2011 Tohoku (Japan) Earthquake

2.1 Introduction

Accumulated data and experiences are very important in the reliable seismic design of structures. However, it is also true that theoretical expectations and predictions are also of significance for the design of extremely important structures and facilities which are influential for the society and wide district. This was demonstrated in the past earthquakes which are very rare from the viewpoint of return period in the same area.

The most devastating earthquake in Japan after the 1923 Great Kanto earthquake hit eastern Japan in the afternoon of March 11, 2011 (see [1], Takewaki [2, 3], Takewaki et al. [4]). The moment magnitude 9.0 earthquake is one of the five most powerful earthquakes in the world since modern record-keeping began in 1900. It was made clear afterward that the recording system for low-frequency and large-amplitude ground motions was not sufficient in Japan and the first preliminary Japan Meteorological Agency (JMA) magnitude was smaller than 8 (7.9 exactly). The JMA magnitude was updated immediately as 8.4. Records of earthquake ground motions outside Japan were then used to determine the exact moment magnitude of 9.0 (intermediate announcement was 8.8). The earthquake resulted from the thrust faulting near the subduction zone plate boundary between the Pacific and North America Plates (AIJ [1], NIED [5], USGS [6]).

Nearly 20,000 people were killed or are still missing by this great earthquake and the ensuing monster tsunami as of November 1, 2011. The principal cause of this devastating result is due to the great tsunami following the large earthquake. Table 2.1 and Fig. 2.1 show the human and economic loss in recent major natural disasters (data from Asahi newspaper [7]). It can be observed that the economic loss in the 2011 off the Pacific coast of Tohoku earthquake is extremely large.

The maximum height (run-up height) of the tsunami was reported to have attained almost 40 m (Miyako City, Iwate Prefecture) and this was observed in the

I. Takewaki et al., *Improving the Earthquake Resilience of Buildings*,
Springer Series in Reliability Engineering, DOI: 10.1007/978-1-4471-4144-0_2,

Table 2.1 Human and economic loss in recent major natural disasters (data from Asahi newspaper [7])

	Number of victims	Economic loss (Billion dollars)
East Japan great earthquake disaster (2011)	20,631	309
Hurricane Katrina (2005)	1,833	135
Hyogoken–Nanbu earthquake (Kobe EQ 1995)	6,437	100
China (2008)	87,476	85
Chile earthquake (2010)	562	30
New Zealand earthquake (2011)	181	13
Haiti earthquake (2010)	222,570	7.8
North Pakistan earthquake (2005)	73,338	5.2
Sumatra earthquake (2004)	165,708	4.5
Cyclone Nargis (Myanmar 2008)	138,366	4.0

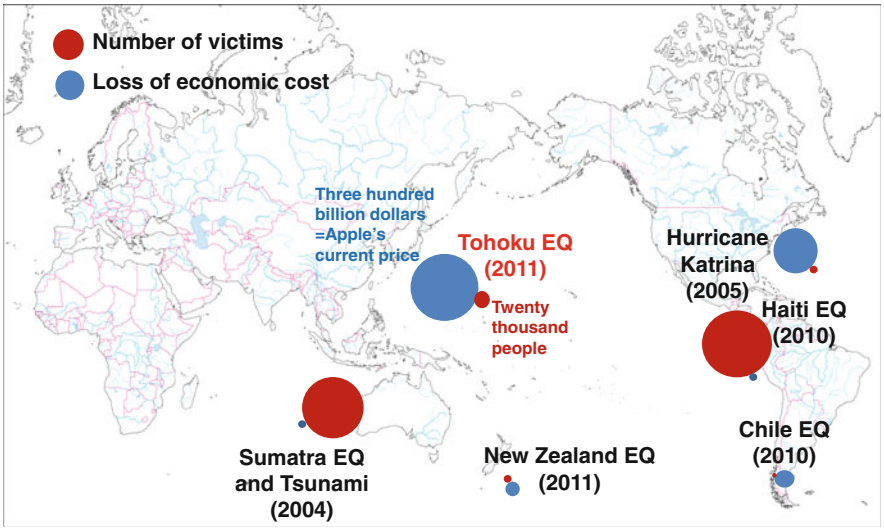

Fig. 2.1 Human and economic loss in recent major natural disasters (data from Asahi newspaper [7])

bay area with complex coast line shapes. It was also reported that the tsunami arrived at the third or fourth story in some buildings and invaded over 5 km from the coastline (Natori City, Miyagi Prefecture). It should be remarked that the number of collapsed (or damaged) buildings and houses remains not clear because most of the damages resulted from the tsunami and a clear record was not left. More detailed data on this earthquake can be obtained from the National Research Institute for Earth Science and Disaster Prevention (NIED) of Japan.

Because super high-rise buildings in mega cities in Japan have never been shaken by the so-called long-period ground motions with high intensities, the response of high-rise buildings to such long-period ground motions is now one of the most controversial issues in the field of earthquake-resistant design in Japan [8]. The issue of long-period ground motion and its effect on building structural design was initially brought up in Mexico, the USA, and Japan during 1980–1990s (for example [9–10]). Some clear observations have actually been reported recently (most famous one is the severe sloshing in oil tanks during the Tokachioki earthquake, Japan in 2003 [11]) and the earthquake ground motions in Tokyo, Yokohama, and Osaka during the March 11, 2011 earthquake are regarded to be extremely influential for super high-rise buildings. In December 2010, just before this earthquake, a set of simulated long-period ground motions was constructed and provided by the Japanese Government [8] for the retrofit of existing high-rise buildings and as a design guideline for new high-rise buildings.

In this chapter, we describe first the characteristics of this 2011 earthquake and discuss the properties of long-period ground motions from the viewpoint of critical excitation, i.e., the phenomenon of resonance characterized by the coincidence of the predominant period of ground motions with the fundamental natural period of high-rise buildings. It is shown that the criticality of the long-period ground motions can be investigated based on the theory of critical excitation [12–14]. This theory is intended to overcome the difficulty resulting from the uncertainty of earthquake ground motions (for example Geller et al. [15]). The credible bounds of input energy responses are obtained using the critical excitation method with the constraints on acceleration and velocity powers. It is demonstrated that the long-period ground motions can be controlled primarily by the velocity power and the ground motion recorded in Tokyo during the 2011 off the Pacific coast of Tohoku earthquake actually included fairly large long-period wave components.

Furthermore, tentatively designed 40- and 60-story steel buildings are subjected to such long-period ground motion as recorded in Shinjuku, Tokyo during the 2011 off the Pacific coast of Tohoku earthquake. It is shown that high-hardness rubber dampers, a kind of viscoelastic dampers with low temperature and frequency dependency, are able to damp the building vibration during long-period ground motions in an extremely shorter duration than in case of the building without those dampers. It is reported recently that this high-hardness rubber damper has a damping performance comparable with oil dampers. Two assumed 40-story steel buildings are also subjected to a set of simulated long-period ground motions taken from a December 2010 document of the Japanese Government [8] for the detailed investigation of response characteristics of super high-rise buildings under many simulated long-period ground motions in various areas.

2.2 General Characteristics of the 2011 Off the Pacific Coast of Tohoku Earthquake

The general characteristics of the 2011 off the Pacific coast of Tohoku earthquake are explained first. The source inversion and slip distribution using near-source strong ground motions are shown in Fig. 2.2a [16]. Since it is necessary to understand the size of the 2011 earthquake, the comparison of slipped fault size is shown in Fig. 2.2b among the 2004 Sumatra earthquake ($M = 9.1$), the 1923 Great Kanto earthquake ($M = 7.9$), the 1995 Hyogoken-Nanbu (Kobe) earthquake ($M = 7.3$), and the 2011 off the Pacific coast of Tohoku earthquake ($M = 9.0$) [17]. Due to the large magnitude and the distance from the source to the Honshu island of Japan, fairly wide areas in the eastern Japan were influenced and shaken by this earthquake.

The representative near-source ground motions along the Pacific coast in the eastern Japan are illustrated from north to south in Fig. 2.3a [18]. It can be found that two or more series (or groups) of waves exist in some areas and most ground motions continue for over 2 min. This implies the repeated occurrence of the fault slips in wide areas. This phenomenon has been pointed out by many researchers (for example Elnashai et al. [19], Hatzigeorgiou and Beskos [20], Moustafa and Takewaki [21]). It was reported afterwards that three main fault slips were observed in this series of events, i.e., the first at the eastern side of Sendai City (off Miyagi Prefecture), the second at the southern (off Miyagi and Fukushima Prefectures) and northern (off Iwate Prefecture) parts of the first one, and the third at the further southern side of the second slip (off Ibaragi Prefecture).

Figure 2.3b presents a more detailed description of those recorded ground motions (Yellow star indicates the epicenter). The following is the interpretation by NIED of Japan [22]. In Tohoku area (from Iwate Prefecture through Fukushima Prefecture), two wave groups (pink and yellow colors) can be observed from the vicinity of the epicenter (star mark). This means that main fault ruptures occurred twice in the vicinity of the epicenter one after another. In Fukushima Prefecture, a wave group (blue color) can be observed around 200 s toward the north. There are intensive waves between the yellow and the blue arrows. In Ibaragi Prefecture, a wave group (blue color arrow downward) can be seen. These results imply that a fault rupture occurred around the epicenter and this rupture induced many subsequent ruptures.

It is believed that the data of ground motions in Fig. 2.3 are very useful for the investigation of the accuracy of methods for constructing the ground motions from several sources. The distributions of the maximum ground accelerations and the maximum ground velocities determined from K-NET and KiK-net (NIED) data are shown in Fig. 2.4 [23].

Table 2.2 shows the top ten largest observed peak ground accelerations during this earthquake [18]. It is found that the maximum ground acceleration over 2.9 g was recorded at the K-NET station of Tsukidate in Kurihara City of Miyagi Prefecture. However, it is reported that the predominant period of this ground

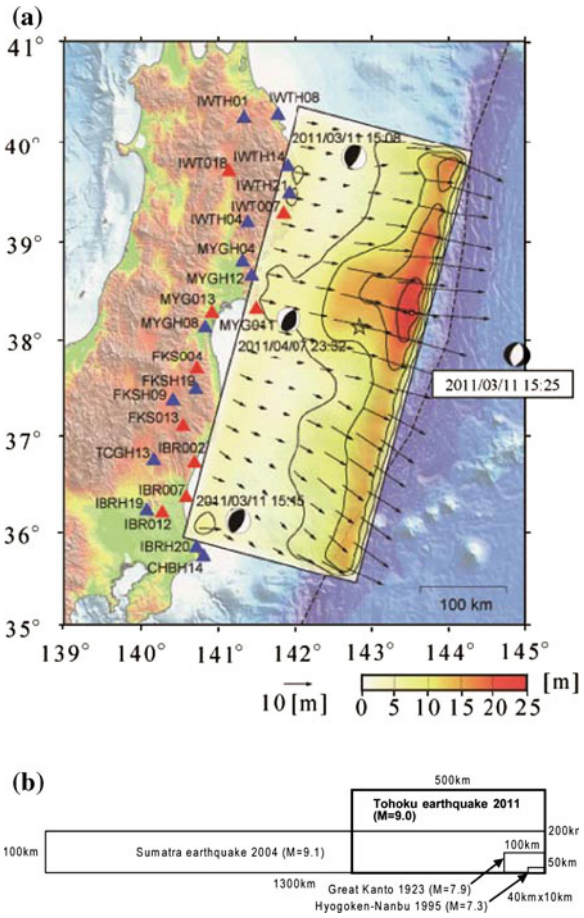

Fig. 2.2 **a** Source inversion and slip distribution using near-source strong ground motions [16], **b** Fault size of 2004 Sumatra earthquake ($M = 9.1$), 1923 Great Kanto earthquake ($M = 7.9$), 1995 Hyogoken-Nanbu (Kobe) earthquake ($M = 7.3$), and 2011 off the Pacific coast of Tohoku earthquake ($M = 9.0$) (data from Asahi newspaper [17]) (Reproduced from Takewaki et al. [4] with kind permission from © Elsevier)

motion is shorter than 0.3 s and this ground motion did not affect most buildings so much. These ground motion characteristics are common in almost all the areas along the Pacific coast in eastern Japan and the damage to buildings is not so large in spite of the tremendous magnitude of 9.0. The damages of most buildings are thought to result from the monster tsunami.

Other peculiar points observed in this 2011 earthquake may be a wide spread of liquefaction and settlement of land along the Pacific coast in Miyagi and Iwate Prefectures. It was reported that remarkable liquefaction occurred in many places on soft grounds including sands (over 42 km^2 even in Tokyo bay area) and the settlement over 1 m of land in Miyagi and Iwate Prefectures may result from the movement of plates near the epicenter. It is understood that the unexpected wide spread of liquefaction in spite of not so high level of maximum ground acceleration results from the long duration of shaking (over 2 min and four times longer than the Hyogoken-Nanbu earthquake). It is thought that this long duration of

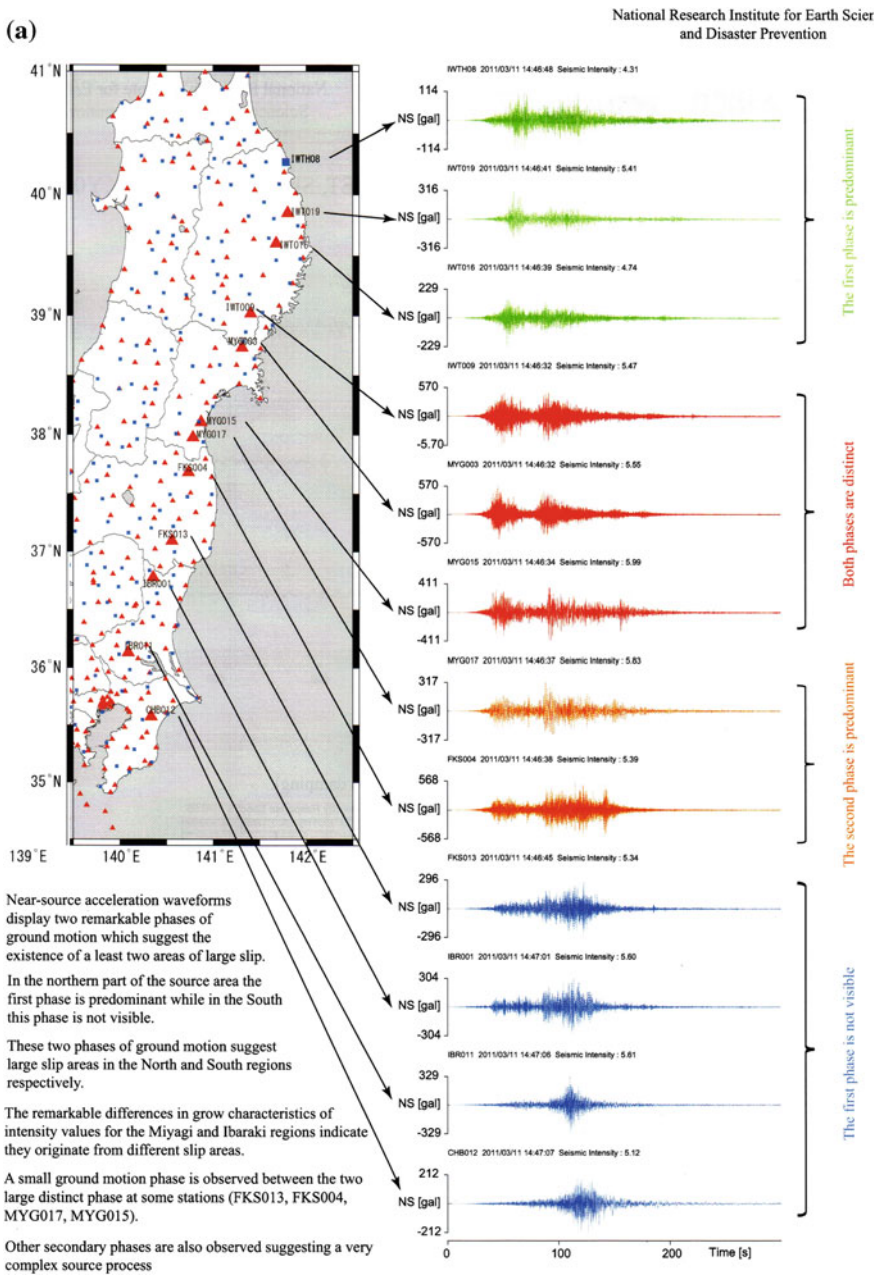

Fig. 2.3 **a** Characteristics of near-source ground motions along Pacific coast in East Japan [18], **b** Relation among fault rupture, wave propagation, and ground motion sequences (*Yellow star* indicates the epicenter) [22]

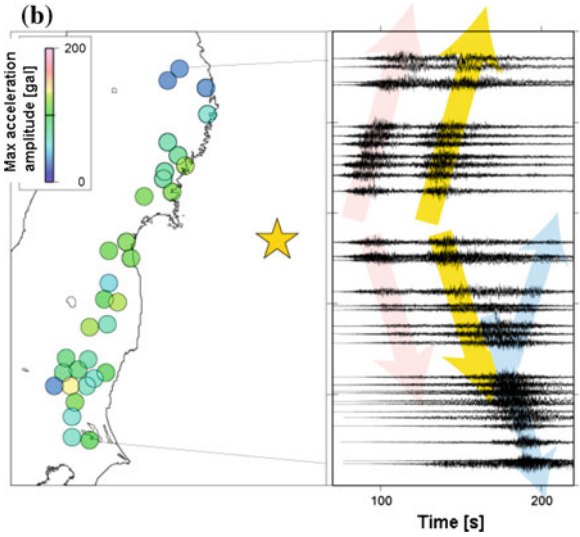

Fig. 2.3 (Continued)

shaking caused a rapid increase of excess pore water pressure. The liquefaction was also observed in Tokyo bay area and it was reported that 14.5 km^2 experienced liquefaction in Urayasu City in Chiba prefecture (one of Tokyo bay area cities).

As stated above, one of the most important issues in mega cities like Tokyo, Osaka, and Nagoya during this 2011 earthquake is the occurrence of long-period ground motions which could affect severely most super high-rise buildings through the resonant phenomenon. It is often reported that many super high-rise buildings in Tokyo and Osaka were severely shaken by those long-period ground motions. This issue will be discussed in the following sections in detail.

2.3 Seismic Response Simulation of Super High-Rise Buildings in Tokyo

2.3.1 Properties of Ground Motions in Tokyo

Figure 2.5a shows the acceleration waveforms of the long-period ground motion recorded at K-NET, Shinjuku station (TKY007) [18] and Fig. 2.5b presents the corresponding velocity wave forms [18]. It can be observed that the maximum ground velocity attains about 0.25 m/s and the ground shaking continues for over several minutes. The velocity response spectra for 1 and 5 % damping are shown in Fig. 2.6 [18]. The corresponding ones of Japanese seismic design code for 5 %

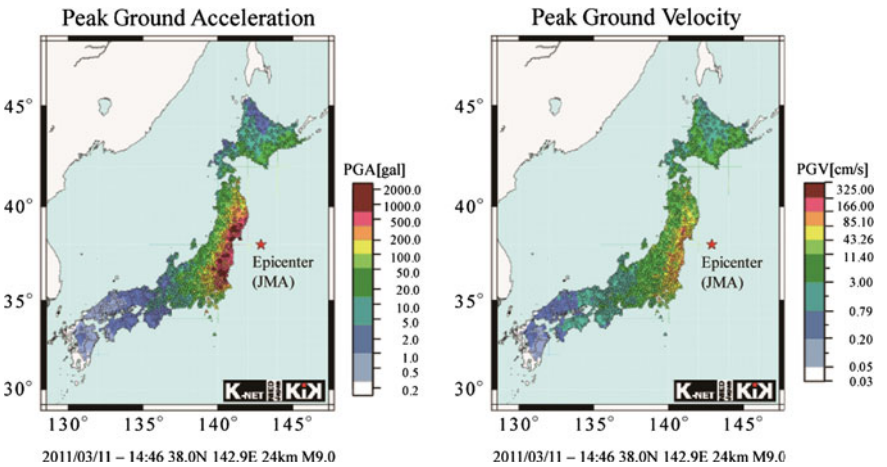

Fig. 2.4 Maximum ground accelerations and maximum ground velocities determined from K-NET and KiK-net data [23]

Table 2.2 List of 10 largest observed peak ground accelerations [18]

	Station name	PGA (gal)	JMA instrumental intensity[a]
1	MYG004	2,933	6.6
2	MYG012	2,019	6.0
3	IBR003	1,845	6.4
4	MYG013	1,808	6.3
5	IBR013	1,762	6.4
6	FKSH10	1,335	6.0
7	TCGH16	1,305	6.5
8	TCG014	1,291	6.3
9	IBRH11	1,224	6.2
10	MYGH10	1,137	6.0

[a] *JMA* Japan Meteorological Agency

MYG Miyagi prefecture, *IBR* Ibaragi prefecture, *FKS* Fukushima prefecture, *TCG* Tochigi prefecture. This list is based on information obtained by March 13, 2011 from 276 K-NET and 112 KiK-net sites

damping are also plotted in Fig. 2.6. It is understood that these ground motions include long-period components up to 10 s. The duration of records at K-NET stations is 300 s and it was found that this duration is not sufficient for the investigation of long-period ground motions.

For investigating further the long-period characteristics of that record, the Fourier amplitude spectra of both acceleration and velocity records have been obtained. Figure 2.7 shows the Fourier amplitude spectra of accelerations of Fig. 2.5a and Fig. 2.8 illustrates those of velocities of Fig. 2.5b [2].

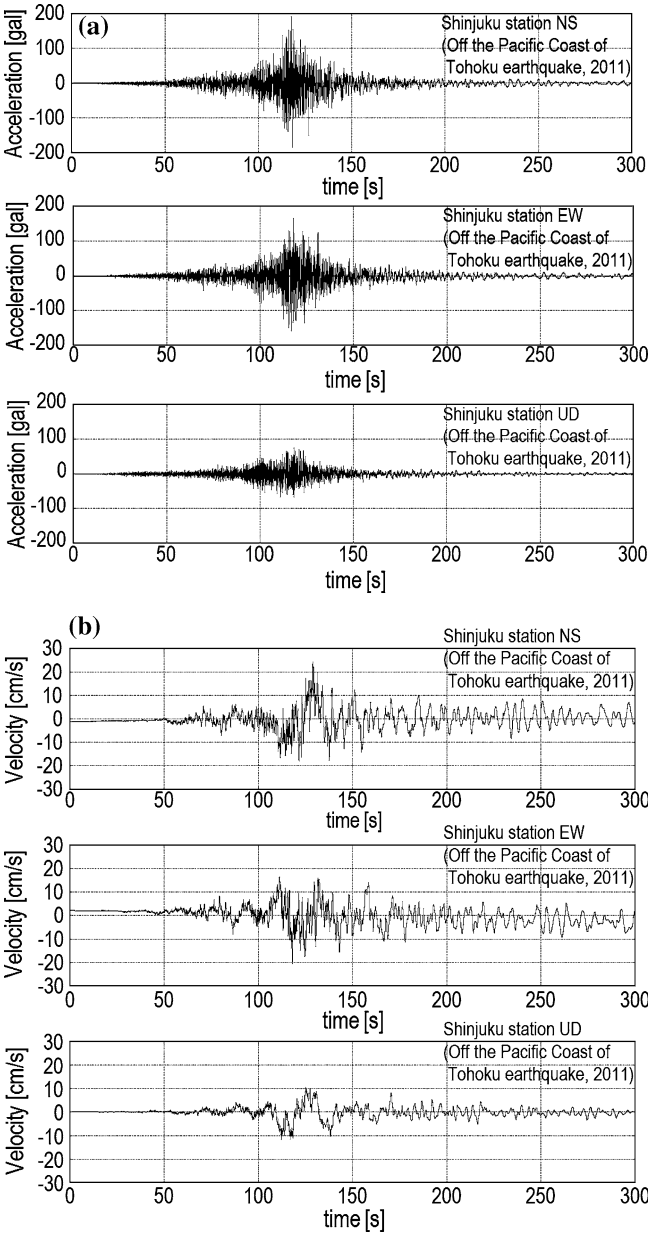

Fig. 2.5 **a** Long-period acceleration ground motion recorded at K-NET, Shinjuku station (TKY007) (Reproduced from Takewaki et al. [4] with kind permission from © Elsevier), **b** Long-period velocity ground motion recorded at K-NET, Shinjuku station (TKY007) (Reproduced from Takewaki et al. [4] with kind permission from © Elsevier)

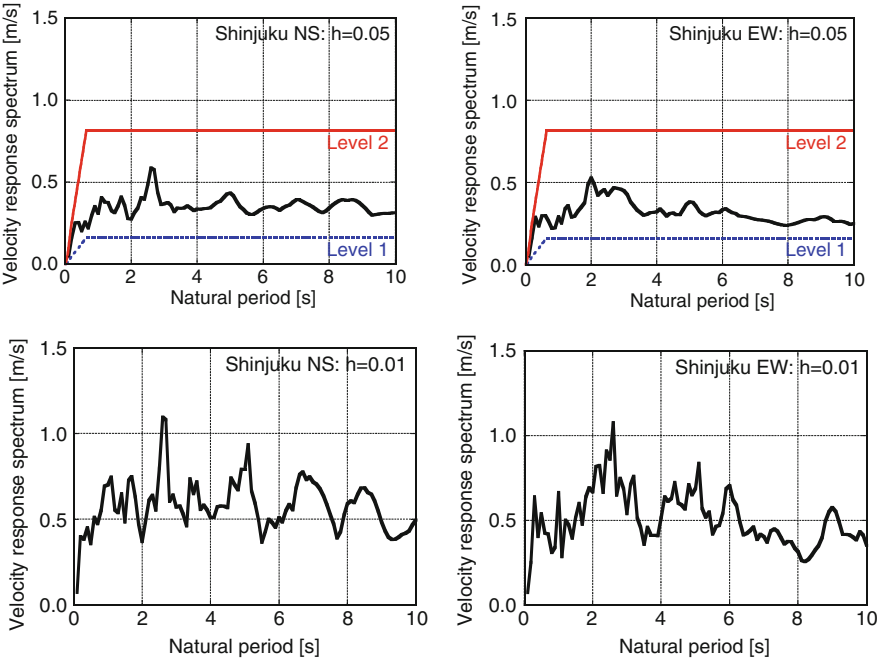

Fig. 2.6 Velocity response spectra (5 and 1 % damping) of ground motions at Shinjuku station (TKY007) and the corresponding ones of Japanese seismic design code for 5 % damping (Reproduced from Takewaki et al. [4] with kind permission from © Elsevier)

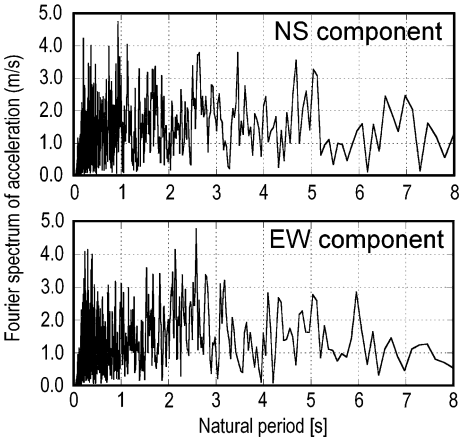

Fig. 2.7 Fourier amplitude spectra of acceleration ground motion at K-NET, Shinjuku station (TKY007) (Reproduced from Takewaki et al. [4] with kind permission from © Elsevier)

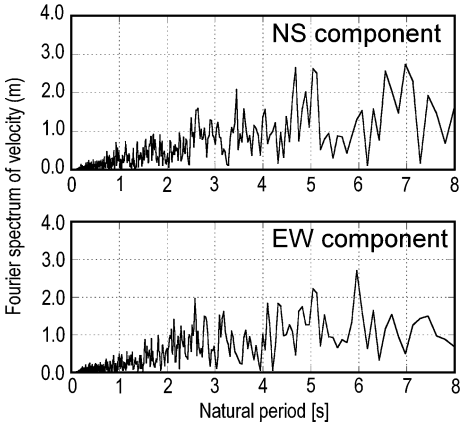

Fig. 2.8 Fourier amplitude spectra of velocity ground motion at K-NET, Shinjuku station (TKY007) (Reproduced from Takewaki et al. [4] with kind permission from © Elsevier)

2.3.2 Measure of Criticality in Long-Period Ground Motions

The critical excitation method [12, 24] is one of the methods for disclosing the level of criticality of ground motions. In the early stage, the maximum displacement was employed as the criticality measure. Then earthquake input energy was introduced to measure the criticality from the view point of input energy [24].

Figure 2.9 explains the schematic diagram for computing credible bounds of the input energy per unit mass E_I/m to a single degree-of-freedom (SDOF) model for acceleration and velocity constraints [13, 14, 24]. The function $F(\omega)$ in the diagram indicates the energy transfer function defined by

$$F(\omega) = \frac{2h\Omega\omega^2}{\pi\{(\Omega^2 - \omega^2)^2 + (2h\Omega\omega)^2\}} \tag{2.1}$$

where Ω: natural circular frequency of the SDOF model, h: damping ratio and ω: the excitation frequency. The input energy per unit mass E_I/m to the SDOF model can then be expressed by

$$E_I/m = \int_0^\infty |A(\omega)|^2 F(\omega)\mathrm{d}\omega \tag{2.2a}$$

or

$$E_I/m = \int_0^\infty |V(\omega)|^2 \omega^2 F(\omega)\mathrm{d}\omega \tag{2.2b}$$

where $A(\omega)$ and $V(\omega)$ are the Fourier transforms of the ground motion acceleration and ground motion velocity, respectively. It can be observed from Fig. 2.9 that the region of short natural period can be controlled by the credible bound for the

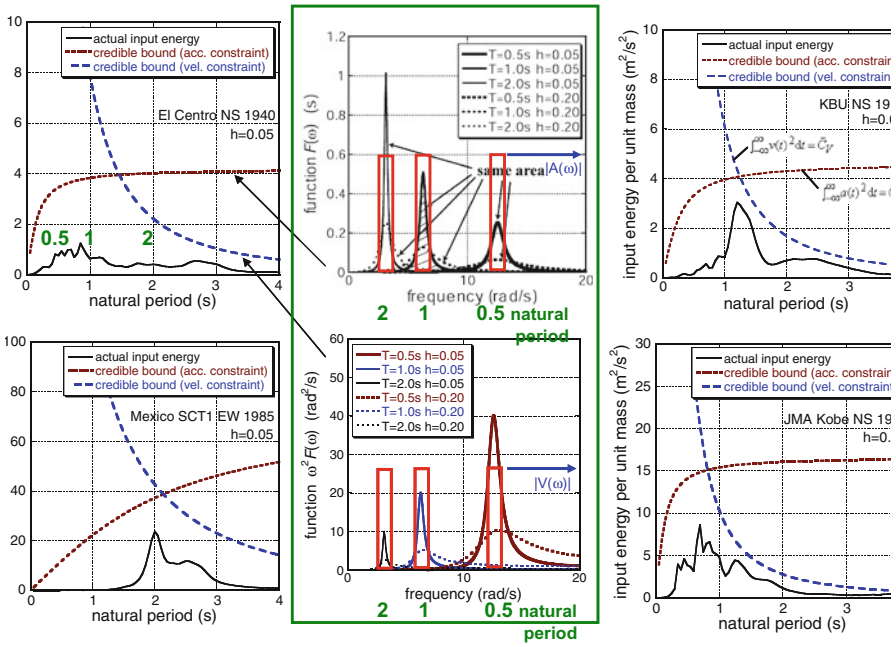

Fig. 2.9 Schematic diagram for computing credible bounds for acceleration and velocity constraints (Reproduced from Takewaki et al. [4] with kind permission from © Elsevier)

acceleration constraint and the region of long period can be controlled by the credible bound for the velocity constraint as explained in [13, 24]. It may be concluded that the introduction of both credible bounds enables the construction of the credible bound with uniform risk in all the natural period range. The word of 'uniform risk' is used in the meaning that the ratio of the actual input energy to the corresponding credible bound is almost constant in some ground motions regardless of the natural period of the model.

Figure 2.10a presents the comparison of the actual input energies (5 % damping), the credible bounds [13, 14, 24] for acceleration constraints (acceleration power in Housner and Jennings [25]) and the credible bounds for velocity constraints (velocity power in Housner and Jennings [25]) for NS and EW components [2]. The intersection point implies the predominant period from the viewpoint of input energy. The periods of 4 and 6 s are such predominant periods of ground motions and this implies that the ground motion recorded at K-NET, Shinjuku station (TKY007) actually included fairly large long-period wave components. For comparison, Fig. 2.10b shows the corresponding figures for El Centro NS 1940 and JMA Kobe NS 1995 (Hyogoken-Nanbu earthquake) [2, 13, 24]. The intersection point corresponds to rather shorter period ranges.

It may be concluded that the credible bound for the velocity constraint can control the bound of input energy from the long-period ground motion and this

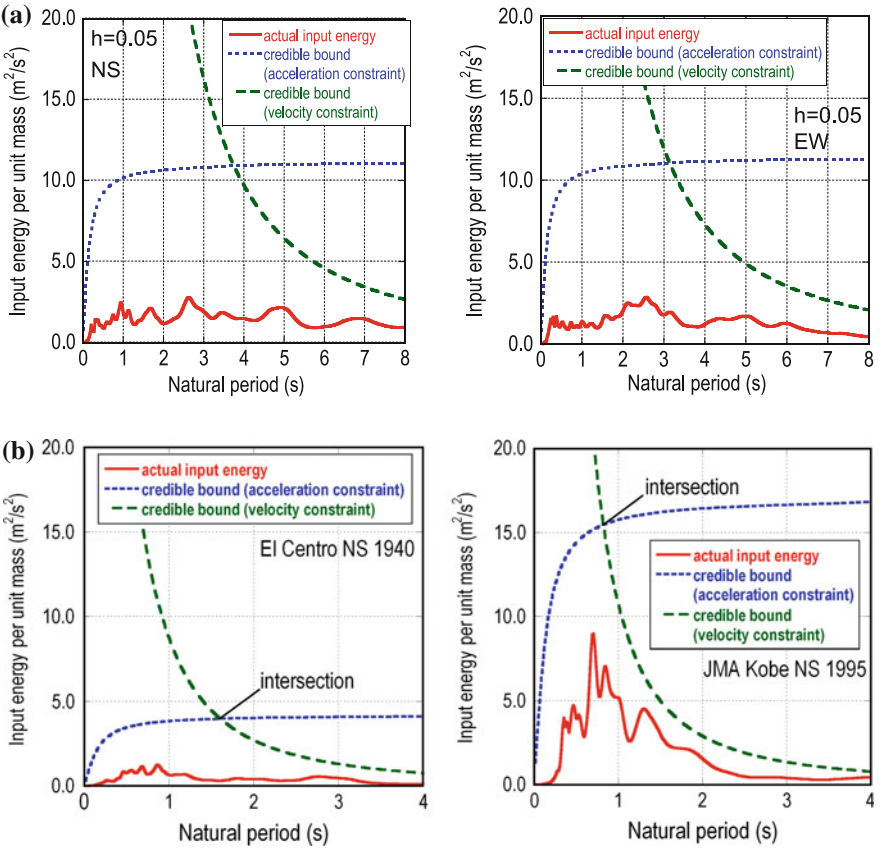

Fig. 2.10 **a** Actual input energies per unit mass (5 % damping), the credible bounds for acceleration constraints and the credible bounds for velocity constraints for the ground motions at K-NET, Shinjuku station (TKY007), **b** Actual input energies per unit mass (5 % damping), the credible bounds for acceleration constraints and the credible bounds for velocity constraints for El Centro NS (1940) and JMA Kobe NS (1995) (Reproduced from Takewaki et al. [4] with kind permission from © Elsevier)

bound plays a role for overcoming the difficulties caused by uncertainties of long-period ground motions (predominant period and intensity level).

2.3.3 Seismic Response Simulation of Super High-Rise Buildings in Tokyo

The 2011 off the Pacific coast of Tohoku earthquake may be the first earthquake to have occurred between tectonic plates and have affected super high-rise buildings

Table 2.3 Cross-sections of members

Story	Column (mm)	Beam (mm)
31–40	600 × 600 × 20 × 20	850 × 300 × 15 × 25
21–30	800 × 800 × 25 × 25	850 × 300 × 15 × 25
11–20	1,000 × 1,000 × 35 × 35	850 × 300 × 20 × 30
1–10	1,000 × 1,000 × 45 × 45	1,000 × 300 × 20 × 40

in mega cities. In order to investigate the influence of the recorded long-period ground motions on high-rise buildings, two steel moment-resisting building frames of 40 and 60 stories have been studied in [2]. The 40-story building has a fundamental natural period of $T_1 = 4.14$ s and the 60-story building has a corresponding one of $T_1 = 5.92$ s.

The buildings have a plan of 40 × 40 m (equally spaced 36 columns; span length = 8 m) and one planar frame is taken as the object frame. The uniform story height is 4 m. The floor mass per unit area is assumed to be 800 kg/m^2. The damping ratio is taken as 0.01 in accordance with the well-accepted database [26]. The variability of damping ratio is large depending on amplitude, building usage, etc. and most of the data exist in 0.5–3.0 % in high-rise steel buildings [26]. Therefore, 1 % damping (most credible one) has been used here. The cross-sectional properties of the 40-story steel building frame are shown in Table 2.3. The composite beam action (stiffening by floor slabs) has been taken into account. The stiffness of beams has been set as 1.5 times the original stiffness. The yield stress of the steel members is 235 N/mm^2. The rigid part of members is introduced at each beam–column connection.

It is well accepted that the passive dampers are very effective in the reduction of earthquake response in high-rise buildings. For the purpose of clarifying the merit of viscoelastic dampers (high-hardness rubber dampers [27]) (see Fig. 2.11), the buildings of 40 and 60 stories without and with these high-hardness rubber dampers have been subjected to the long-period ground motion recorded at K-NET, Shinjuku station (TKY007). The outline of the high-hardness rubber dampers is shown in Fig. 2.11. One damper unit consists of rubber thickness = 15 mm and rubber area = 0.96 m^2. The frame includes four damper units at every story.

Figure 2.12 shows the maximum story displacements and interstory drifts of the 40-story building of $T_1 = 4.14$ s without or with high-hardness rubber dampers to ground motion at Shinjuku station (TKY007) (frame response: elastic or elastic–plastic) [2]. It can be understood that linear and nonlinear analyses provide nearly the same results in this case. On the other hand, Fig. 2.13 illustrates the maximum story displacements and interstory drifts of the 60-story building of $T_1 = 5.92$ s without or with high-hardness rubber dampers to ground motion at Shinjuku station (TKY007) (frame response: elastic–plastic, 'four dampers per story' corresponds to 'damper double') [2]. Only nonlinear analyses have been performed. It can be observed that high-hardness rubber dampers are effective for the reduction of displacements.

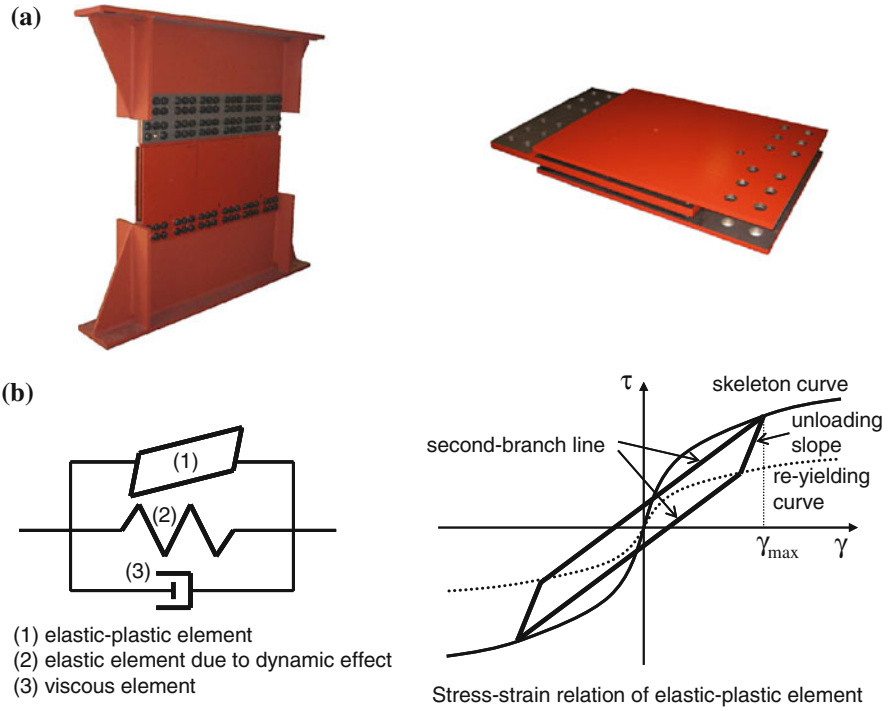

Fig. 2.11 High-hardness rubber dampers **a** Overview, **b** Modeling into three elements (Reproduced from Takewaki et al. [4] with kind permission from © Elsevier)

Table 2.4 shows the comparison of the maximum absolute accelerations at the top between the 60-story buildings without and with high-hardness rubber dampers under three recorded ground motions (EW component of TKY007, EW component at Chiyoda-ku station near Shinjuku station and NS component at Osaka WTC) during the 2011 off the Pacific coast of Tohoku earthquake. It can be seen that the top acceleration is reduced by the introduction of the high-hardness rubber dampers.

Figure 2.14a presents the comparison of time histories of top-story displacements of the assumed 60-story building of $T_1 = 5.92$ s to ground motion at Shinjuku station (EW component of TKY007) during the 2011 off the Pacific coast of Tohoku earthquake (frame response: elastic–plastic, without or with high-hardness rubber dampers) [2]. It can be understood that the high-hardness rubber dampers can damp the building vibration in an extremely short duration. It should be remarked that this ground motion was recorded for 300 s (records at K-NET stations are recorded for 300 s as a rule) and the response after 300 s is a free vibration in this case. Figure 2.14b shows a similar comparison to ground motion (EW component) at Chiyoda-ku station near Shinjuku station during the 2011 off the Pacific coast of Tohoku earthquake. It can be understood that the longer ground

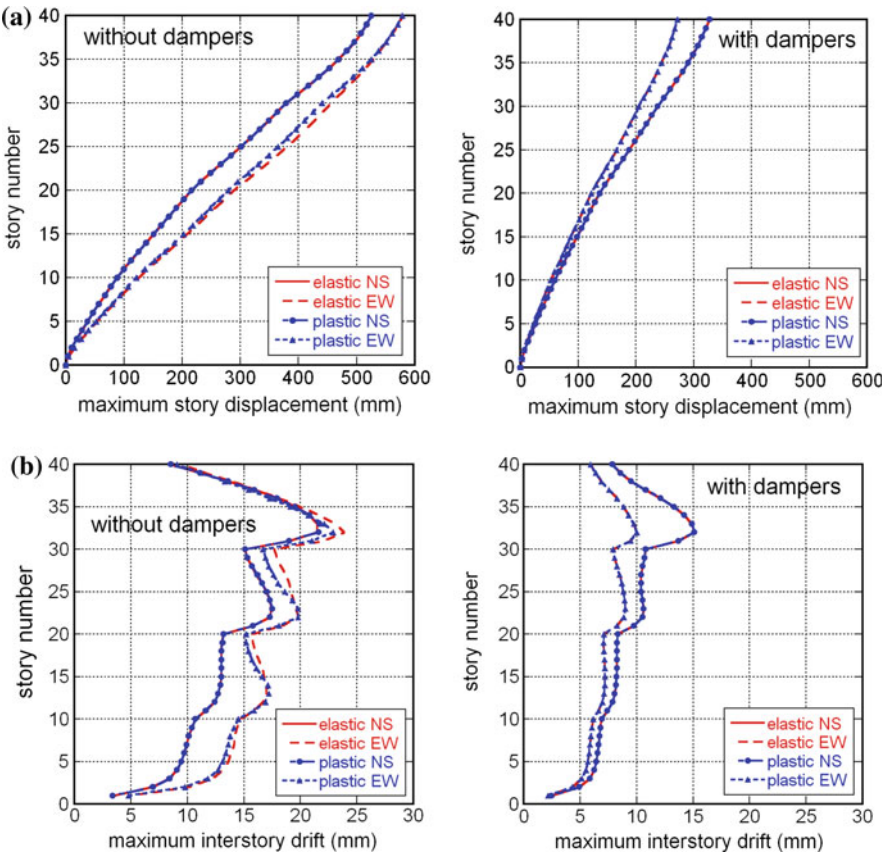

Fig. 2.12 **a** Maximum story displacement and **b** maximum interstory drift of a 40-story building of $T_1 = 4.14$ s without or with high-hardness rubber dampers to ground motion at Shinjuku station (TKY007) during the 2011 off the Pacific coast of Tohoku earthquake (frame response: elastic or elastic–plastic) (Reproduced from Takewaki et al. [4] with kind permission from © Elsevier)

motion duration of 600 s can demonstrate well the damping performance of the high-hardness rubber dampers.

It has been reported [28] that a 54-story building [height = 223 m: fundamental natural period = 6.2 s (short-span direction), 5.2 s (long-span direction)] retrofitted with passive oil dampers including the supporting bracing system in Shinjuku, Tokyo experienced a top displacement of 0.54 m during the 2011 off the Pacific coast of Tohoku earthquake. The vibration duration has been reported to be over 13 min. It has also been found that the building would have attained a top displacement of 0.7 m if the passive dampers had not been installed. This fact corresponds well to the result explained above.

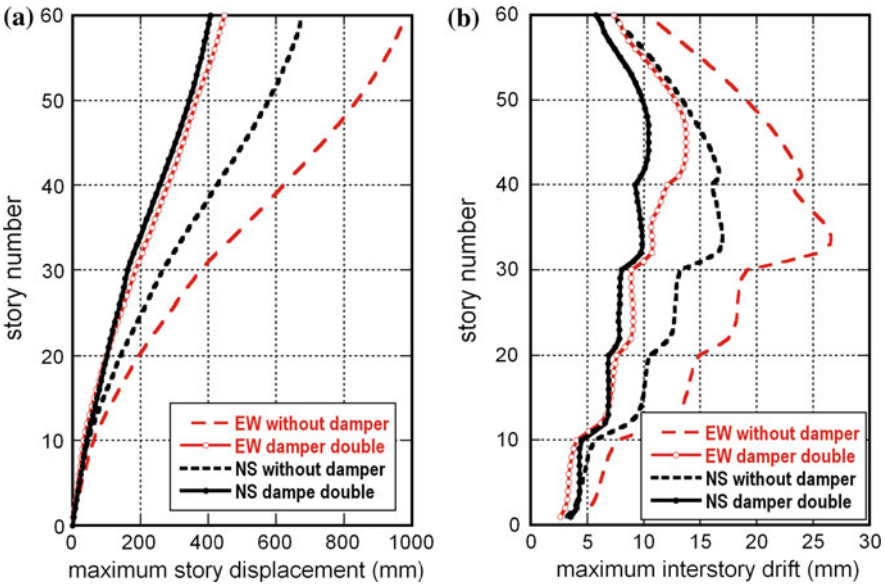

Fig. 2.13 **a** Maximum story displacement and **b** maximum interstory drift of a 60-story building of $T_1 = 5.92$ s without or with high-hardness rubber dampers to ground motion at Shinjuku station (TKY007) during the 2011 off the Pacific coast of Tohoku earthquake (frame response: elastic–plastic, '4 dampers per story' corresponds to 'damper double') (Reproduced from Takewaki et al. [4] with kind permission from © Elsevier)

Table 2.4 Reduction of top acceleration via high-hardness rubber dampers (m/s^2)

60-story building	EW component of TKY007	EW component at Chiyoda-ku station	NS component at Osaka WTC
No damper	1.79	1.54	0.933
With damper	1.65	1.21	0.667

There is another report that a 55-story super high-rise building in Osaka [height = 256 m: fundamental natural period = 5.8 s (long-span direction), 5.3 s (short-span direction)] was shaken severely regardless of the fact that Osaka is located far from the epicenter (about 800 km) and the JMA instrumental intensity was three in Osaka. It should be pointed out that the level of velocity response spectra of ground motions observed here (first floor) is almost the same as that at the Shinjuku station (K-NET) in Tokyo and the top-story displacement are about 1.4 m (short-span direction) and 0.9 m (long-span direction). Figure 2.15a shows the ground acceleration, ground velocity and top-story displacement. It can be observed that a clear resonant phenomenon occurs during about eight cycles. The corresponding velocity response spectra of the ground motion are shown in Fig. 2.15b. The resonance phenomenon can be explained by using the structure of

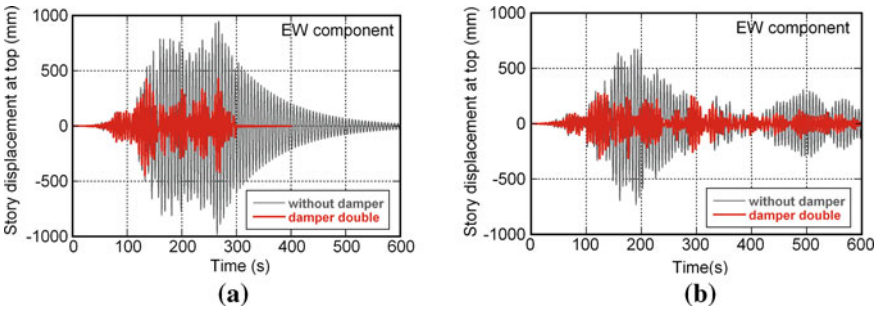

Fig. 2.14 **a** Comparison of time histories of top-story displacement of an assumed 60-story building of $T_1 = 5.92$ s without or with high-hardness rubber dampers to ground motion at Shinjuku station (EW component of TKY007) during the 2011 off the Pacific coast of Tohoku earthquake (frame response: elastic–plastic) (Reproduced from Takewaki et al. [4] with kind permission from © Elsevier), **b** Comparison of time histories of top-story displacement of an assumed 60-story building of $T_1 = 05.92$ s without or with high-hardness rubber dampers to ground motion (EW component) at Chiyoda-ku station near Shinjuku station during the 2011 off the Pacific coast of Tohoku earthquake (frame response: elastic–plastic) (Reproduced from Takewaki et al. [4] with kind permission from © Elsevier)

the surface ground in Fig. 2.15c. Figure 2.15d illustrates the comparison of the actual input energies (5 % damping), the credible bounds [13, 14, 24] for acceleration constraints (acceleration power in Housner and Jennings [25]) and the credible bounds for velocity constraints (velocity power in Housner and Jennings [25]) for NS and EW components [2]. It can be seen that the ground motion recorded here in Osaka bay area actually included fairly large long-period wave components. These facts imply the need of consideration of long-period ground motions in the seismic resistant design of super high-rise buildings in mega cities even though the site is far from the epicenter. The seismic retrofit using hysteretic steel dampers and oil dampers is being planned.

Figure 2.16 illustrates the comparison of the sensitivity of the response amplification in the resonant case and nonresonant case with respect to damping reduction. It may be useful to note that the amplification by damping can be expressed by

$$1/2h \quad \text{for resonant long-period ground motion} \tag{2.3a}$$

$$1.5/(1+10h) \text{ for non-resonant conventional ground motion} (\text{ratio to } h = 0.05) \tag{2.3b}$$

This implies that the high sensitivity of the response to damping in resonant long-period ground motions. Since the damping ratio in super high-rise buildings is usually small (smaller than 0.02), this high sensitivity may be kept in mind in their structural design.

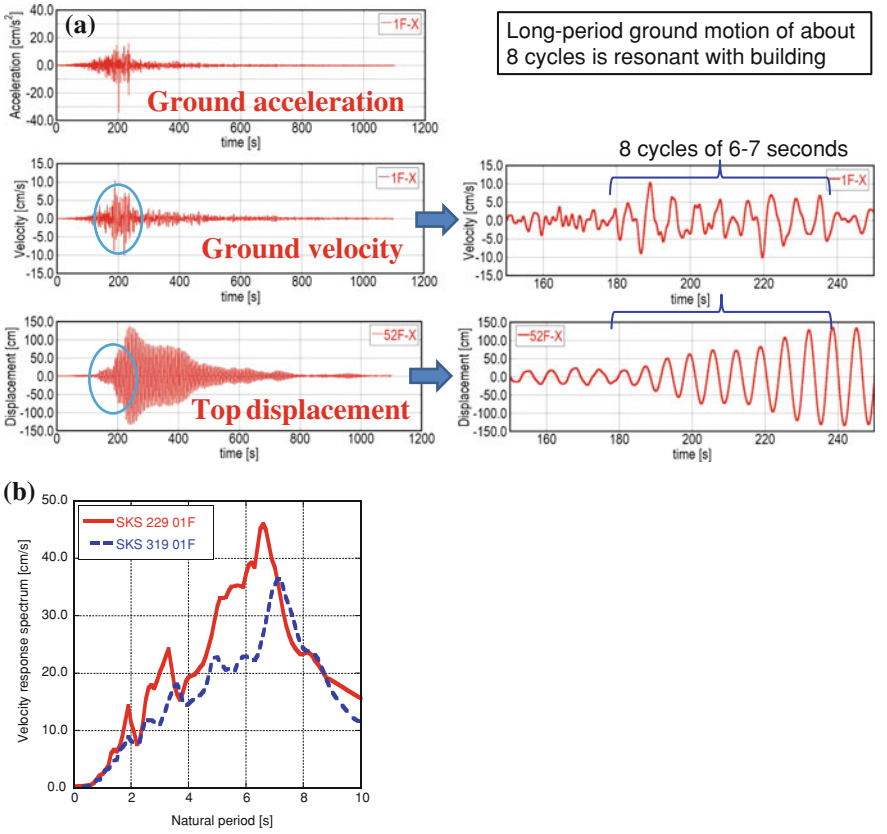

Fig. 2.15 **a** Ground acceleration, ground velocity and top-story displacement of a 55-story building in Osaka during the 2011 off the Pacific coast of Tohoku earthquake, **b** Velocity response spectra of ground motion (horizontal two directions, 229: NS, 319: EW), **c** Shear wave velocity distribution of surface ground, **d** Actual input energies per unit mass (5 % damping), the credible bounds for acceleration constraints and the credible bounds for velocity constraints for the ground motions in Osaka bay area

2.4 Seismic Response of High-Rise Buildings to Simulated Long-Period Ground Motions (Japanese Government Action)

2.4.1 Characteristics of Simulated Long-Period Ground Motions

On December 21, 2010, the Japanese Government made a press release to upgrade the regulation for high-rise buildings under long-period ground motions. The Ministry of Land, Infrastructure, Transport and Tourism (MLIT) of Japan specified

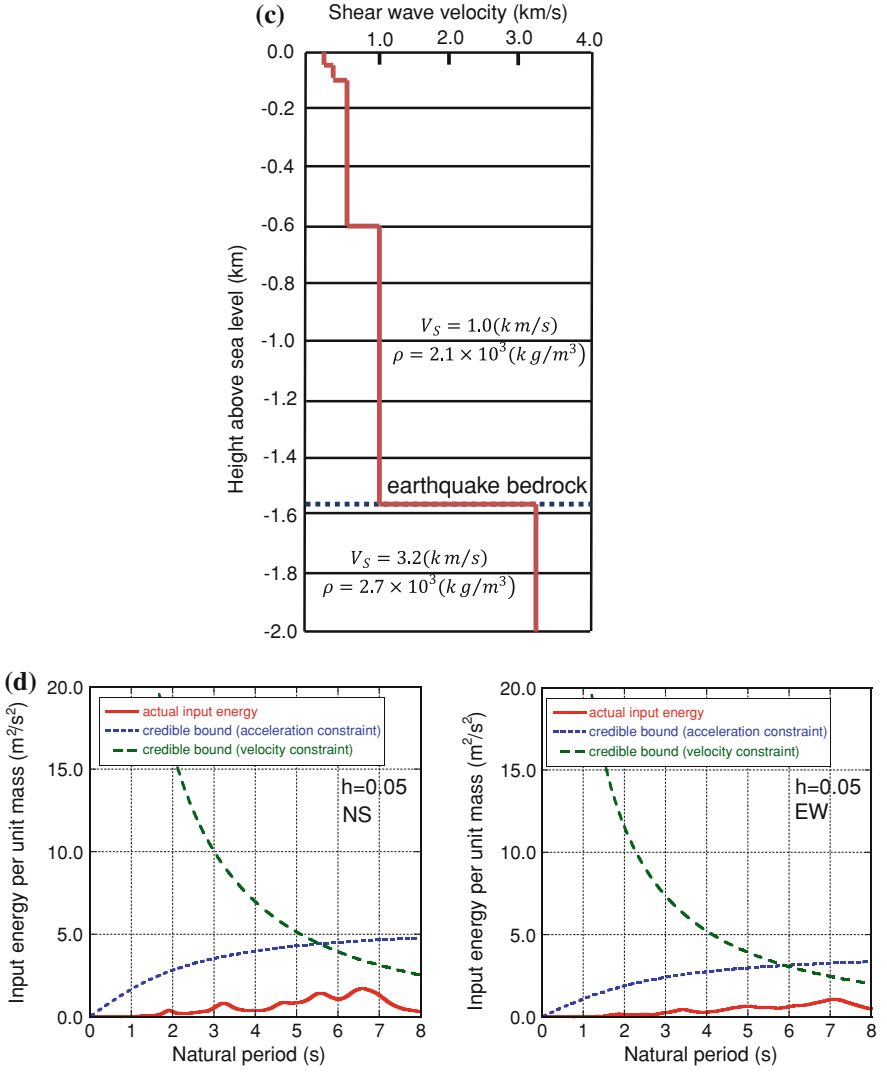

Fig. 2.15 (Continued)

nine areas in Tokyo, Nagoya, and Osaka (see Fig. 2.17) [8]. Areas 1–4 exist in Tokyo, Areas 5–7 in Nagoya, and Areas 8, 9 in Osaka.

Figure 2.18a shows the acceleration and velocity records of simulated ground motions in those nine areas specified in Fig. 2.17. These simulated ground motions were generated by using the acceleration response spectra (5 %) at the bedrock and the group delay time (mean and standard deviation) for the phase property [8]. It can be observed that large velocity waves appear in later times.

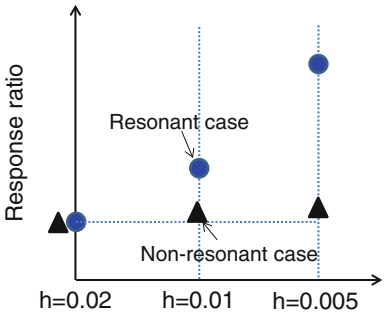

Fig. 2.16 Comparison of sensitivities of the response amplification in the resonant case and nonresonant case with respect to damping reduction

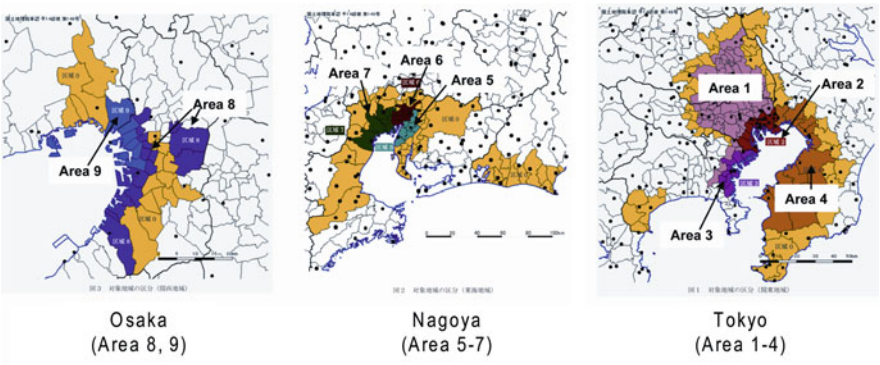

Fig. 2.17 Nine areas in Osaka, Nagoya, and Tokyo specified by the MLIT of Japan MLIT [8] (Reproduced from Takewaki et al. [4] with kind permission from © Elsevier)

Figure 2.18b presents the pseudo velocity response spectra and velocity response spectra of the simulated acceleration ground motions specified by the MLIT. It can be seen that the velocity spectra in 2–8 s have relatively large magnitudes.

Figure 2.18c shows the actual input energies per unit mass [13, 24, 23], the credible bounds for acceleration constraints [13, 24] and the credible bounds for velocity constraints [13, 24] for the simulated ground motions specified by the MLIT. As stated before, the intersection point indicates the predominant period of the ground motion. As in the ground motion recorded at K-NET, Shinjuku station (TKY007), 3–8 s are such predominant periods and this implies that the simulated ground motions actually include fairly large long-period wave components.

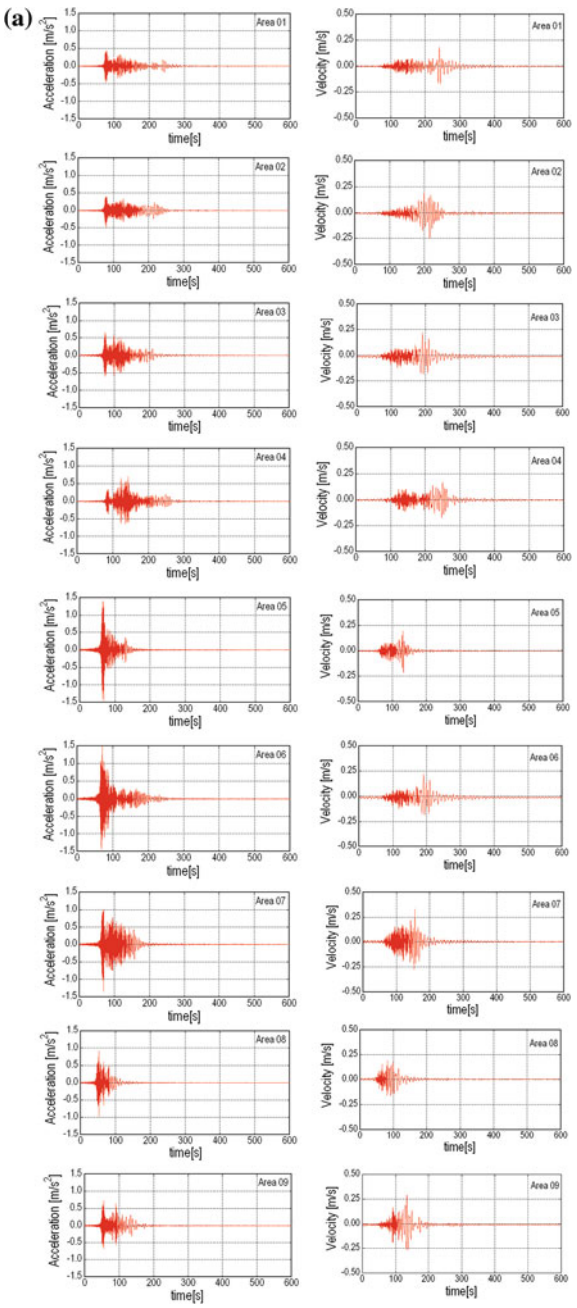

Fig. 2.18 **a** Acceleration and velocity ground motion records at nine areas specified by the MLIT of Japan (data from MLIT [8]) (Reproduced from Takewaki et al. [4] with kind permission from © Elsevier), **b** Pseudo velocity response spectra (5 % damping) and velocity response spectra of the simulated acceleration ground motions specified by the MLIT of Japan MLIT [8] (Reproduced from Takewaki et al. [4] with kind permission from © Elsevier), **c** Actual input energies per unit mass (5 % damping), the credible bounds for acceleration constraints and the credible bounds for velocity constraints for the simulated ground motions specified by the MLIT of Japan (Reproduced from Takewaki et al. [4] with kind permission from © Elsevier)

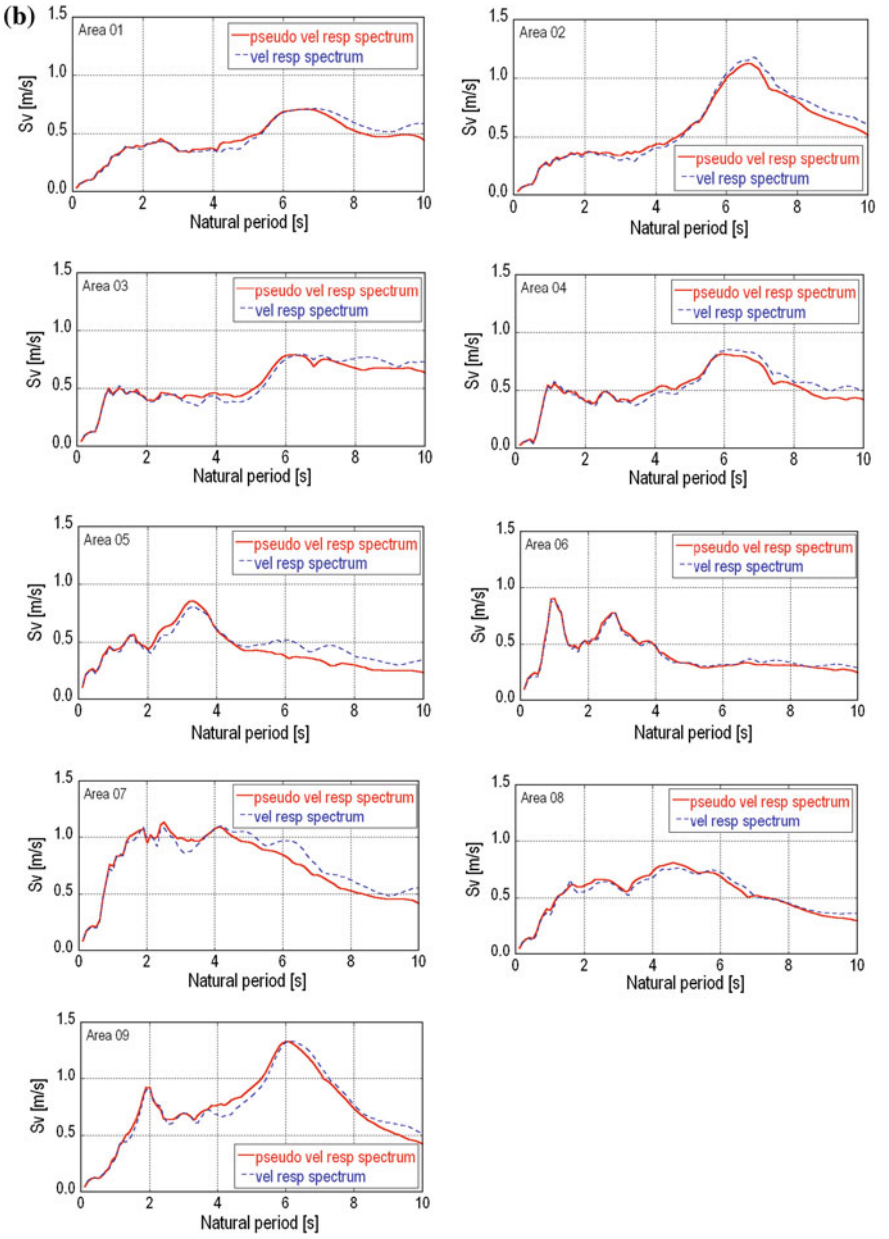

Fig. 2.18 (Continued)

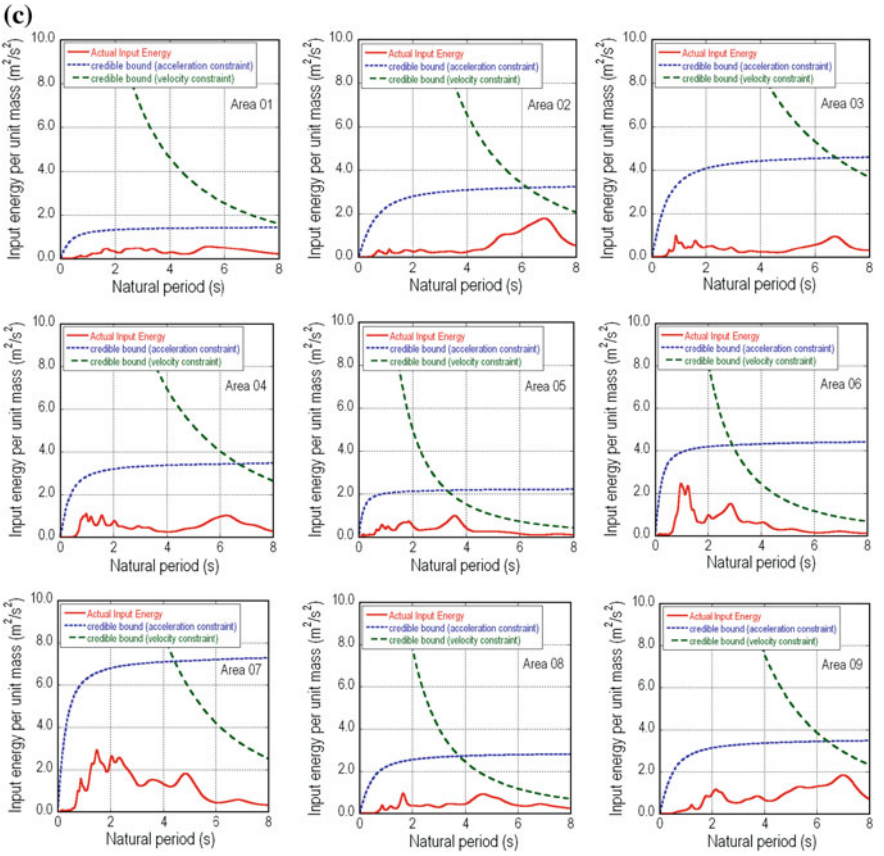

Fig. 2.18 (Continued)

2.4.2 Response Simulation of Super High-Rise Buildings Without and With High-Hardness Rubber Dampers

In order to investigate the influence of the simulated ground motions in Areas 1–9 on the response of high-rise buildings, two buildings of 40 stories have been assumed. The parameters of the buildings are the same as those stated in Sect. 2.3.3. The stiffness of beams has been evaluated as double the original stiffness for the building frame of $T_1 = 3.6$ s and as 1.5 times the original stiffness for the building frame of $T_1 = 4.14$ s. Judging from the database on the relationship of the building height with its fundamental natural period in Japan, the model of $T_1 = 3.6$ s is a slightly stiff building model for 40-story steel buildings and the model of $T_1 = 4.14$ s is a slightly flexible steel building model. Only the latter has been treated in Sect. 2.3. For the purpose of clarifying the merit of viscoelastic dampers [high-hardness rubber dampers [27] as in the previous case], the buildings

of 40 stories without and with these high-hardness rubber dampers have been subjected to the simulated long-period ground motions. One damper unit consists of rubber thickness = 15 mm and rubber area = 0.96 m^2. 'Damper single' includes two damper units at every story and 'damper double' includes four damper units at every story.

Figure 2.19a illustrates the comparison of the time histories of the top displacement of the 40-story buildings of $T_1 = 3.6$ s without and with high-hardness rubber dampers (frame response; elastic) under a simulated long-period ground motion in Area 5 (Nagoya area). It can be observed that the high-hardness rubber dampers are able to damp the building vibration during long-period ground motions in an extremely shorter duration compared to the building without those dampers.

Figure 2.19b explains the mechanism of response amplification under long-period ground motion. It can be found that remarkable building response amplification begins almost after the end of input acceleration and such amplification corresponds well with the velocity wave.

Figure 2.20 presents the time histories of the top displacement of the 40-story buildings of $T_1 = 3.6$ s without and with high-hardness rubber dampers (frame response; elastic) under simulated long-period ground motions in nine areas. It can be found that the responses in Areas 5 and 7 (Nagoya area) are large. Figure 2.21 shows the maximum interstory drifts of the 40-story buildings of $T_1 = 3.6$ s without and with high-hardness rubber dampers (frame response; elastic). It can also be understood that the maximum response of the damper double is not different much from that of the damper single and the damper single is sufficient for the maximum response reduction in this case. However, as for the reduction rate of the vibration, the damper double is better than the damper single.

Figure 2.22 illustrates the time histories of the top displacement of the 40-story buildings of $T_1 = 4.14$ s without and with high-hardness rubber dampers (frame response; elastic). It can be seen that the responses are quite different from those of $T_1 = 3.6$ s shown in Fig. 2.20. This characteristic may depend on the relation of the fundamental natural period of the building with the predominant period of ground motions in nine areas. Figure 2.23 shows the maximum interstory drifts of the 40-story buildings of $T_1 = 4.14$ s without and with high-hardness rubber dampers (frame response; elastic). Different from the case for $T_1 = 3.6$ s shown in Fig. 2.21, the maximum response of the damper double is much smaller than that of the damper single especially in Area 7 which shows the maximum response. This indicates the superiority of the increase of damper quantity in the reduction of the maximum response in addition to the reduction rate of the vibration.

Figure 2.24 presents the comparison of the top displacements of the 40-story buildings of $T_1 = 3.6$ s (elastic or elastic–plastic, without or with dampers) under the simulated long-period ground motion in Area 5. It can be observed that the elastic–plastic response of the building frame decreases the response level to some extent. However, it can also be seen that the high-hardness rubber dampers can damp the vibration so quickly. It has been confirmed that this quick vibration reduction rate can be achieved also by viscous dampers like oil dampers so long as

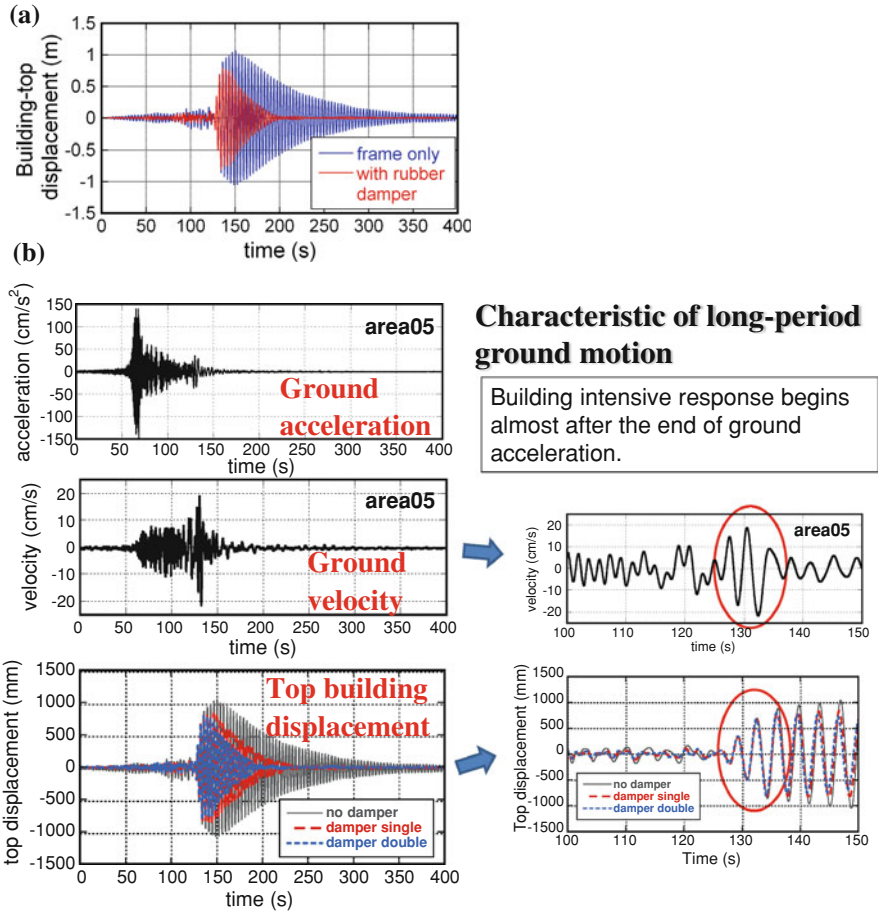

Fig. 2.19 **a** Comparison of the time histories of the top displacement of the 40-story buildings of $T_1 = 3.6$ s without and with high-hardness rubber dampers (frame response; elastic) under a simulated long-period ground motion in Area 5 (Reproduced from Takewaki et al. [4] with kind permission from © Elsevier) **b** Mechanism of response amplification under long-period ground motion

an appropriate amount of dampers is provided. Figure 2.25 shows the maximum interstory drifts of 40-story buildings of $T_1 = 3.6$ s (Area 5) and $T_1 = 4.14$ s (Area 7) without high-hardness rubber dampers (elastic or elastic–plastic). As in Fig. 2.24, it can be seen that the elastic–plastic response of the building frame decreases the response level to some extent. Since the plastic deformation may cause some problems in the beam–column connections (as observed during Northridge and Hyogoken–Nanbu earthquakes) and member plastic deformation capacities, a more detailed investigation will be necessary on the overall characteristics of this property. Figure 2.26 illustrates the plastic hinge formation

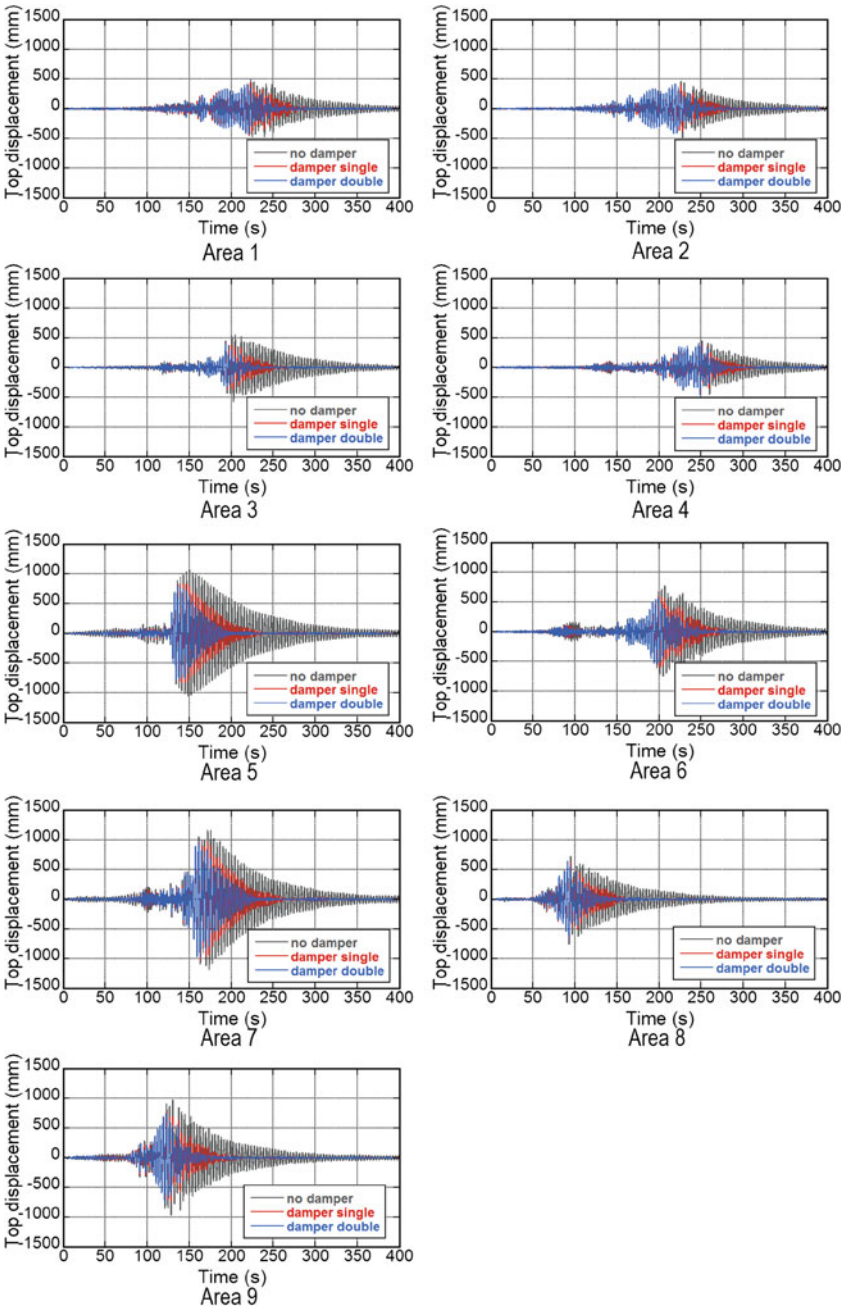

Fig. 2.20 Time histories of top displacement of 40-story buildings of $T_1 = 3.6$ s without and with high-hardness rubber dampers (frame response; elastic) (Reproduced from Takewaki et al. [4] with kind permission from © Elsevier)

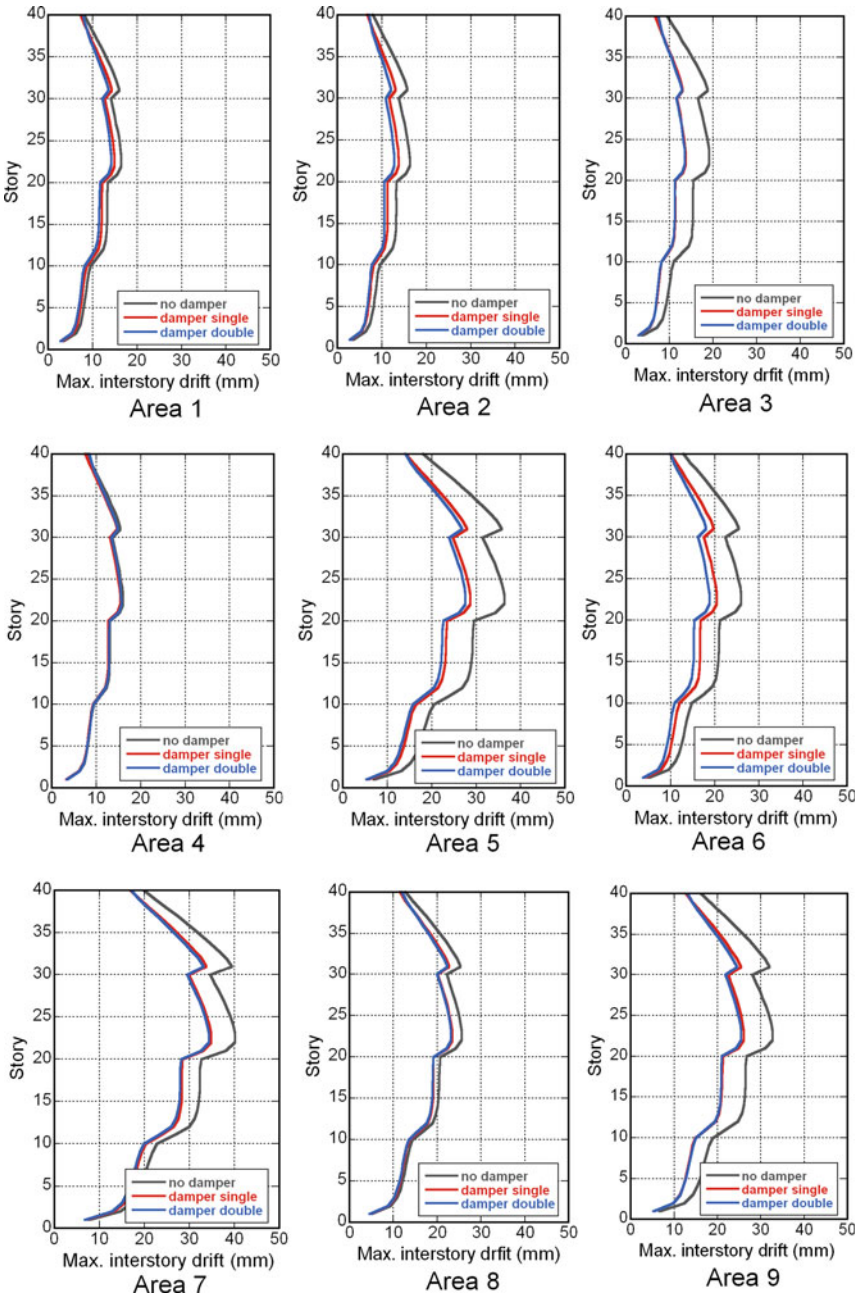

Fig. 2.21 Maximum interstory drifts of 40-story buildings of $T_1 = 3.6$ s without and with high-hardness rubber dampers (frame response; elastic) (Reproduced from Takewaki et al. [4] with kind permission from © Elsevier)

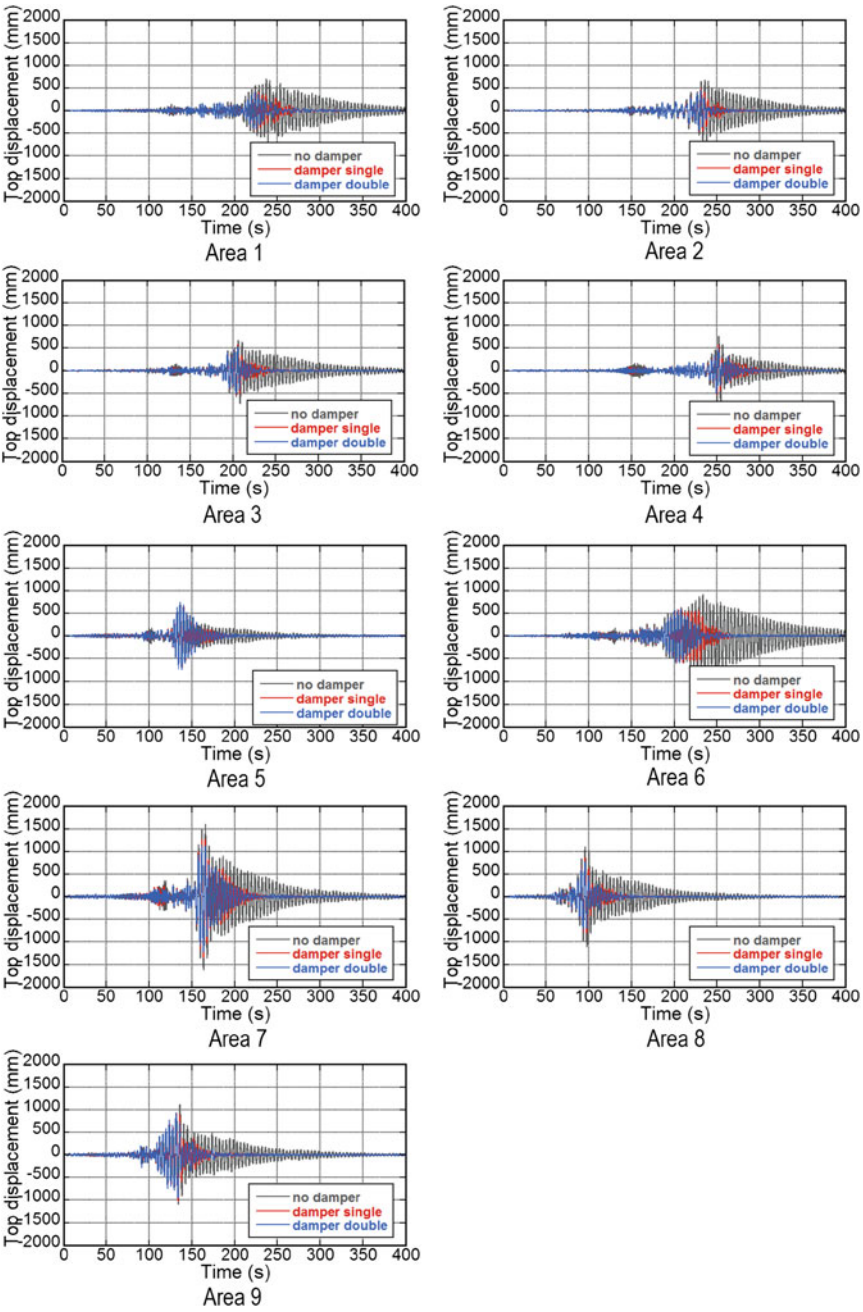

Fig. 2.22 Time histories of top displacement of 40-story buildings of $T_1 = 4.14$ s without and with high-hardness rubber dampers (frame response; elastic) (Reproduced from Takewaki et al. [4] with kind permission from © Elsevier)

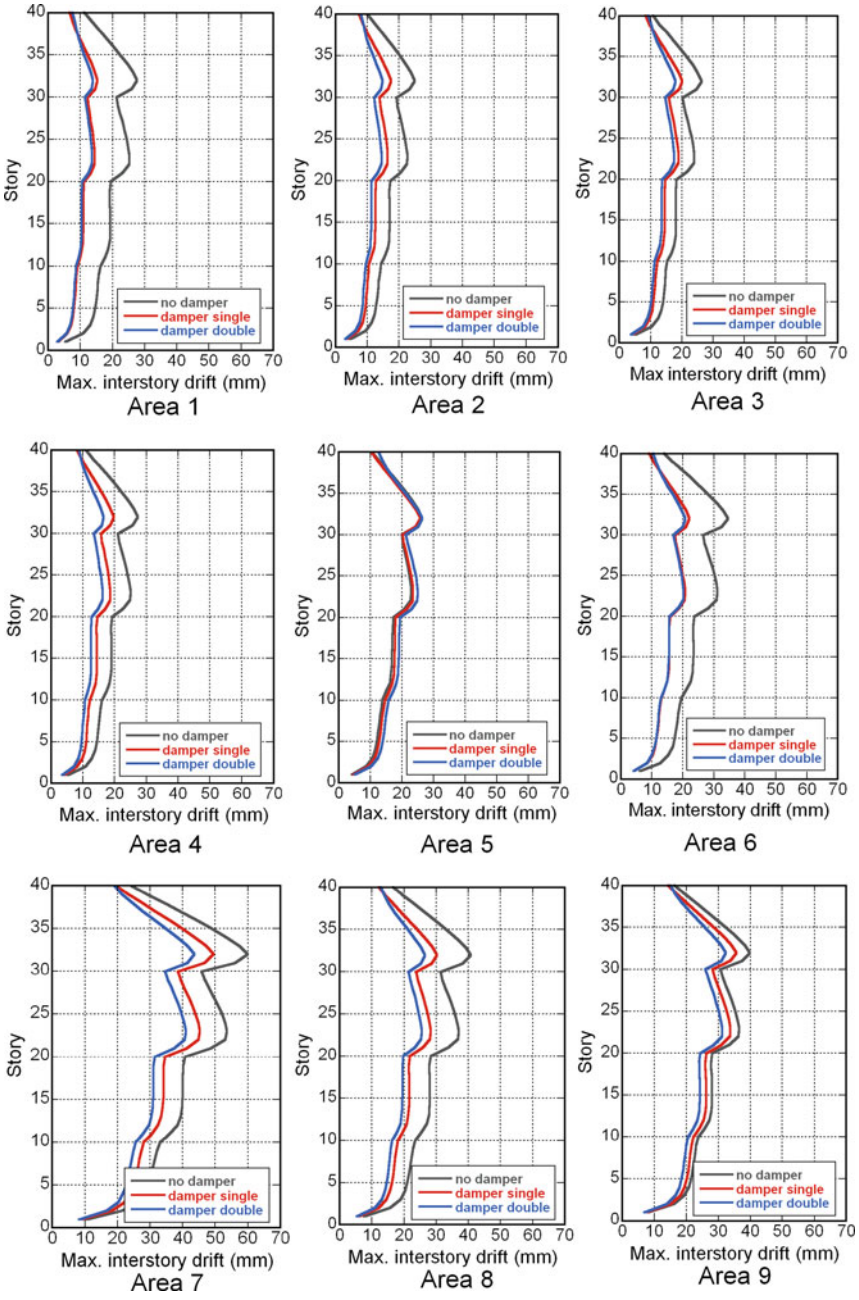

Fig. 2.23 Maximum interstory drifts of 40-story buildings of $T_1 = 4.14$ s without and with high-hardness rubber dampers (frame response; elastic) (Reproduced from Takewaki et al. [4] with kind permission from © Elsevier)

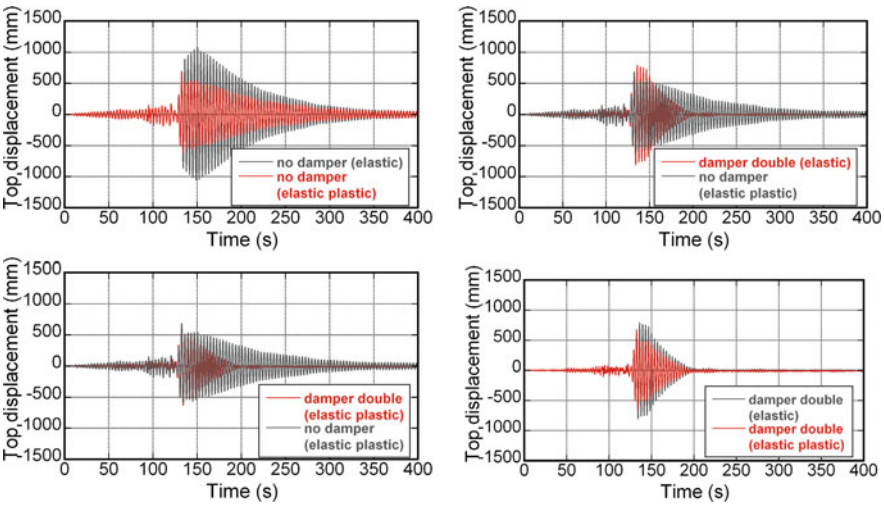

Fig. 2.24 Top displacement of 40-story buildings of $T_1 = 3.6$ s without and with high-hardness rubber dampers (frame response: elastic or elastic–plastic) (Area 5) (Reproduced from Takewaki et al. [4] with kind permission from © Elsevier)

diagram of the building frames without and with dampers. The nonlinear analyses performed take into account both material and geometrical nonlinearities.

The purposes of this chapter (Sect. 2.4) are to disclose the general properties of the effect of simulated long-period ground motions on the responses of high-rise buildings and to investigate the effect of high-hardness rubber dampers in the vibration reduction of high-rise buildings under long-period ground motions. For these purposes only elastic responses have been investigated comprehensively at first (Figs. 2.20, 2.21, 2.22, 2.23). This treatment is valid when high strength steels are used (this is often the case now in Japan), because the response will be almost within the elastic limit. However, since it seems to be also useful to investigate the effect of elastic–plastic behavior on the resonant phenomenon, the comparison between elastic and elastic–plastic responses have been conducted for the model of $T_1 = 3.6$ s in Area 5 and that of $T_1 = 4.14$ s in Area 7 as representative ones. As can be seen from Fig. 2.20, most of the responses are within the elastic limit except in a few cases including Areas 5 and 7. Furthermore, it was made clear that most responses of high-rise buildings in Japan (Tokyo and Osaka) during the 2011 off the Pacific coast of Tohoku earthquake are within the elastic limit. It seems reasonable to a limited extent also from these viewpoints to deal with the elastic response of high-rise buildings under simulated long-period ground motions.

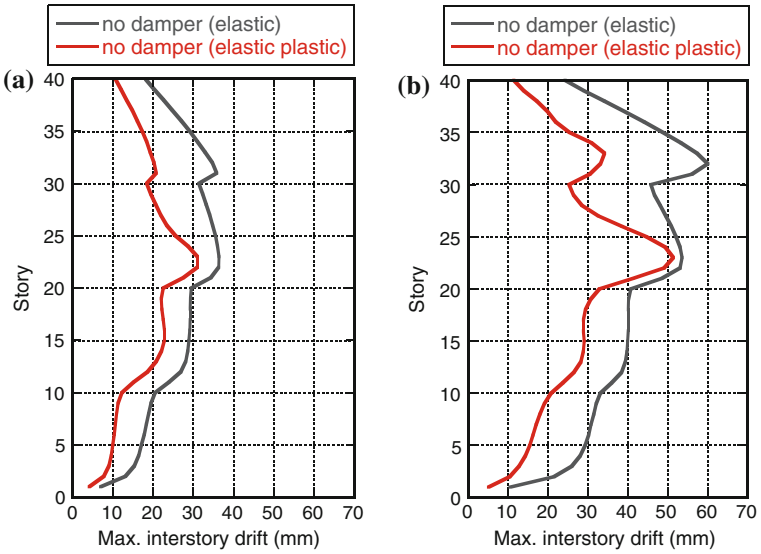

Fig. 2.25 Maximum interstory drifts of 40-story buildings of $T_1 = 3.6$ s and $T_1 = 4.14$ s without high-hardness rubber dampers (frame response; elastic or elastic–plastic), **a** 40-story building of $T_1 = 3.6$ s in area 5, **b** 40-story building of $T_1 = 4.14$ s in area 7 (Reproduced from Takewaki et al. [4] with kind permission from © Elsevier)

2.4.3 AIJ's Research Result

Architectural Institute of Japan (AIJ) made a press release on March 4, 2011 just 1 week before the March 11, 2011 earthquake on the result of their research on the response of high-rise buildings under long-period ground motions [29]. The conclusions in this press release may be summarized as follows:

1. High-rise buildings in Tokyo, Nagoya, and Osaka may experience long-duration vibration under simulated long-period ground motions obtained as a sequence of Tokai, Tonankai, and Nankai earthquakes [30]. However, the collapse will not occur (the possibility may be very low).
2. The long-period ground motions exhibit different properties in different areas. The high-rise buildings also have different properties depending on their heights and constructed periods. The relation of the structural properties of high-rise buildings with the properties of long-period ground motions plays a key role in the evaluation of seismic response of high-rise buildings.
3. The damage to non-structural components, facilities, and furniture may be caused easily. Such damage can be reduced effectively by introducing appropriate steps.
4. Passive dampers will be able to damp the building vibration remarkably and reduce the damage to structural members.

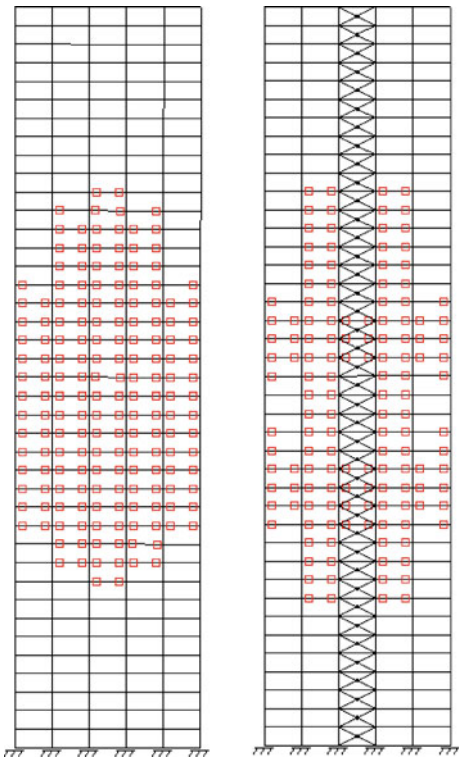

Fig. 2.26 Plastic hinge formation in 40-story buildings of $T_1 = 3.6$ s without and with high-hardness rubber dampers (Area 5) (Reproduced from Takewaki et al. [4] with kind permission from © Elsevier)

2.5 Summary

1. The 2011 off the Pacific coast of Tohoku earthquake is the most devastating earthquake in Japan after the 1923 Great Kanto earthquake in terms of the damaged area and loss cost. This earthquake may be the largest interplate earthquake which attacked mega cities after the construction of super high-rise buildings. However, it is reported that this earthquake may not be the most influential one to be taken into account because the influence depends on the plate (including epicenter) on which mega cities lie and on the soil condition supporting buildings. This fact has been confirmed from the comparison with the result using the simulated ground motions provided by the Japanese Government in December 2010.
2. The ground motion recorded at K-NET, Shinjuku station (TKY007), Tokyo during the 2011 off the Pacific coast of Tohoku earthquake contains fairly large long-period wave components and has a frequency content of broad band (2–6 s). This can be observed from not only the velocity response spectra (and Fourier spectra) but also the earthquake input energy spectra taking into account of the concept of critical excitation. This characteristic has also been

demonstrated by the simulated ground motions provided by the Japanese Government in December 2010.

3. The region of short natural period in the input energy spectrum can be controlled by the credible bound for the acceleration constraint and the region of long period can be controlled by the credible bound for the velocity constraint as demonstrated in the references [13, 14]. The introduction of both credible bounds enables the construction of the credible bound with uniform risk (almost constant ratio of the input energy to its credible bound) in all the natural period range in some ground motions. The credible bound introduced in the references [13, 14] for the velocity constraint can control the bound of input energy from the long-period ground motion and this bound plays a key role for overcoming the difficulties induced by uncertainties of long-period ground motions.
4. Viscoelastic dampers, such as high-hardness rubber dampers, and viscous dampers, such as oil dampers, are able to reduce the building vibration during long-period ground motions in an extremely shorter duration compared to the building without those dampers. It has been made clear from this March 11, 2011 earthquake that the safety is not the only target and the functionality together with the consideration of psychologic aspects (relief) of residents has to be maintained appropriately.
5. The word 'unexpected incident' is often used in Japan after this great earthquake. It may be true that the return period of this class of earthquakes at the same place could be 500–1000 years and the use of this word may be acceptable to some extent from the viewpoint of the balance between the construction cost and the safety level. However, the critical excitation method is expected to enhance the safety level and earthquake resilience of building structures against undesirable incidents drawn from this irrational concept in the future.

References

1. Architectural Institute of Japan (2011) Preliminary reconnaissance report on the 2011 off the Pacific coast of Tohoku earthquake, 6 April 2011 (in Japanese)
2. Takewaki I (2011) Preliminary report of the 2011 off the Pacific coast of Tohoku earthquake. J Zhejiang Univ-SCI A 12(5):327–334
3. Takewaki I (2011) The 2011 off the Pacific coast of Tohoku earthquake and its impact on building structural design, keynote paper (Plenary speaker) at the ASEM11+Congress, in Seoul, Korea, 18–23 Sept 2011
4. Takewaki I, Murakami S, Fujita K, Yoshitomi S, Tsuji M (2011) The 2011 off the Pacific coast of Tohoku earthquake and response of high-rise buildings under long-period ground motions. Soil Dyn Earthq Eng 31(11):1511–1528
5. NIED (2011) National research institute for earth science and disaster prevention. 2011 Off the Pacific Coast of Tohoku earthquake. (in Japanese) Available from http://www.hinet.bosai.go.jp/topics/off-tohoku110311/. Accessed on 3 May 2011
6. USGS (2011) Magnitude 9.0—Near the East coast of Honshu, Japan. Available from http://earthquake.usgs.gov/earthquakes/eqinthenews/2011/usc0001xgp/#summary. Accessed on 3 May 2011

7. Asahi newspaper (2011) 7 Aug 2011 (in Japanese)
8. Ministry of Land, Infrastructure, Transport and Tourism (MLIT) (2011) Code draft for the retrofit of existing high-rise buildings and design guideline for new high-rise buildings. 21 Dec 2010 (in Japanese) Available from http://www.mlit.go.jp/report/press/house05_hh_000218.html. Accessed on 11 Jan 2011
9. Heaton T, Hall J, Wald D, Halling M (1995) Response of high-rise and base-isolated buildings to a hypothetical M 7.0 blind thrust earthquake. Science 267:206–211
10. Ariga T, Kanno Y, Takewaki I (2006) Resonant behavior of base-isolated high-rise buildings under long-period ground motions. Struct Des Tall Spec Buildings 15(3):325–338
11. Zama S, Nishi H, Yamada M, Hatayama K (2008) Damage of oil storage tanks caused by liquid sloshing in the 2003 Tokachi Oki earthquake and revision of design spectra in the long-period range. In: Proceedings of the 14th world conference on earthquake engineering, Beijing, China, 12–17 Oct 2008
12. Drenick RF (1970) Model-free design of aseismic structures. J Eng Mech Div, ASCE 96(EM4):483–493
13. Takewaki I (2004) Bound of earthquake input energy. J Struct Eng, ASCE 130(9):1289–1297
14. Takewaki I (2008) Critical excitation methods for important structures, invited as a semi-plenary speaker. EURODYN 2008, Southampton, England, 7–9 July 2008
15. Geller RJ, Jackson DD, Kagan YY, Mulargia F (1997) Earthquakes cannot be predicted. Science 275:1616
16. NIED (2011) National research institute for earth science and disaster prevention. 2011 off the Pacific Coast of Tohoku earthquake. Source inversion and slip distribution using near-source strong ground motions. (in Japanese) (revised version in 12 April 2011 by Suzuki W, Aoi M and Sekiguchi H) Available from http://www.kyoshin.bosai.go.jp/kyoshin/topics/TohokuTaiheiyo_20110311/inversion/. Accessed on 3 May 2011
17. Asahi newspaper (2011) 10 April 2011 (in Japanese)
18. NIED (2011) National research institute for earth science and disaster prevention. 2011 Off the Pacific Coast of Tohoku earthquake, strong ground motion, emergency meeting of headquarters for earthquake research promotion, 13 March 2011. Available from http://www.k-net.bosai.go.jp/k-net/topics/TohokuTaiheiyo_20110311/nied_kyoshin2e.pdf. Accessed on 20 April 2011
19. Elnashai A, Bommer JJ, Martinez-Pereira A (1998) Engineering implications of strong motion records from recent earthquakes. In: Proceedings of 11th European conference on earthquake engineering. CD-ROM, Paris
20. Hatzigeorgiou GD, Beskos DE (2009) Inelastic displacement ratios for SDOF structures subjected to repeated earthquakes. Eng Struct 31(13):2744–2755
21. Moustafa A, Takewaki I (2011) Response of nonlinear single-degree-of-freedom structures to random acceleration sequences. Eng Struct 33:1251–1258
22. NIED (2011) National research institute for earth science and disaster prevention. 2011 off the Pacific Coast of Tohoku earthquake: overview (in Japanese). Available from http://www.hinet.bosai.go.jp/topics/off-tohoku110311/. Accessed on 3 May 2011
23. NIED (2011) National research institute for earth science and disaster prevention. 2011 off the Pacific coast of Tohoku earthquake, strong ground motion. (in Japanese) Available from http://www.kyoshin.bosai.go.jp/kyoshin/topics/html20110311144626/main_20110311144626.html. Accessed on 20 April 2011
24. Takewaki I (2006) Critical excitation methods in earthquake engineering. Elsevier, Amsterdam
25. Housner GW, Jennings PC (1975) The capacity of extreme earthquake motions to damage structures. In: Hall WJ (ed) Structural and geotechnical mechanics. Prentice-Hall, Englewood Cliff, pp 102–116
26. Satake N, Suda K, Arakawa T, Sasaki A, Tamura Y (2003) Damping evaluation using full-scale data of buildings in Japan. J Struct Eng, ASCE 129(4):470–477

27. Tani T, Yoshitomi S, Tsuji M, Takewaki I (2009) High-performance control of wind-induced vibration of high-rise building via innovative high-hardness rubber damper. Struct Des Tall Spec Buildings 18(7):705–728
28. Asahi newspaper (2011) evening edition of 19 April 2011 (in Japanese)
29. Architectural Institute of Japan (AIJ) (2011) Report at the open research meeting on design guide for super high-rise buildings under long-period ground motions. 4 March 2011 (in Japanese)
30. Kamae K, Kawabe H, Irikura, K (2004) Strong ground motion prediction for huge subduction earthquakes using a characterized source model and several simulation techniques. In: Proceedings of the 13th WCEE, Vancouver

http://www.springer.com/978-1-4471-4143-3

Improving the Earthquake Resilience of Buildings
The worst case approach
Takewaki, I.; Moustafa, A.; Fujita, K.
2013, XVI, 324 p., Hardcover
ISBN: 978-1-4471-4143-3